Influence of wave-function updates in GW calculations on titanates

Gijae Kang, Youngho Kang, and Seungwu Han*
Department of Materials Science and Engineering and Research Institute of Advanced Materials, Seoul National University, Seoul 151-755, Korea

(Received 3 September 2014; revised manuscript received 27 February 2015; published 23 April 2015)

We investigate quasiparticle band structures of rutile and anatase phases of TiO_2 and cubic $SrTiO_3$ using various levels of GW approximations such as G_0W_0, GW_0, GW, $QPGW_0$, and $QPGW$. It is found that the quasiparticle band gap increases as the self-consistency level is ratcheted up from G_0W_0 to GW_0 and GW, and the GW results overestimate the band gap by ∼50% in comparison with the experimental values. Interestingly, when the wave functions are updated in $QPGW_0$ and $QPGW$, the band gap is significantly reduced, which is opposite to the tendency known for other materials. The experimental band gap is most closely reproduced by $QPGW_0$ within ∼10% error. We explain the improvement by the wave-function update in terms of the local change in the charge density, which is different at Ti and O sites and reduces the quasiparticle energy gap.

DOI: 10.1103/PhysRevB.91.155141 PACS number(s): 71.15.−m, 71.20.Nr, 81.05.Hd

I. INTRODUCTION

Titanates such as titanium dioxide (TiO_2) and strontium titanate ($SrTiO_3$) have been studied for several decades due to the central roles in energy and electronic applications [1–5]. For example, TiO_2 is utilized for photocatalytic water splitting because of its long-term stability, nontoxicity, and the adequate band-edge position for hydrogen reduction [2,6,7]. It is also one of the key materials in photovoltaic cells, notably in dye-sensitized solar cells [3,8–11]. On the other hand, $SrTiO_3$ is regarded as "silicon" in oxide electronics owing to its high mobility and facile n-type doping. The simple cubic structure of $SrTiO_3$ is also allowed for high-quality epitaxial interfaces, among which $LaAlO_3/SrTiO_3$ is receiving recent attention due to the unexpected conductivity, magnetism, and superconductivity [12–17]. The high dielectric constants ($\gtrsim$100) of rutile TiO_2 and $SrTiO_3$ also lead to the application to dielectrics in microelectronic devices [18–21].

The band gaps of titanate is the key parameter defining the working principle underlying each application mentioned above. As such, any theoretical effort dealing with titanates should be able to reproduce the experimental band gap if it aims at quantitative analysis or prediction. However, the conventional first-principles methods based on the density functional theory (DFT) is limited in describing the electronic structure due to the self-interaction error and the lack of derivative discontinuity [22–24]. Specifically, in the case of rutile TiO_2, the band gap calculated within the generalized-gradient approximation (GGA) is 1.88 eV, which is much smaller than ∼3.3 eV in experiment [25]. The DFT calculations on anatase TiO_2 and $SrTiO_3$ also suffer from similar errors [26,27]. Consequently, material properties such as light absorption and band-edge position are inaccurate in DFT, undermining the reliability of, for example, computed defect formation energies or magnetic behaviors under impurity doping, in which the precise description of band edge and defect level is essential [28,29].

To overcome the limitation of conventional DFT in calculating the band gap, the GW approximation has been widely employed. In the GW approximation, the self-energy operator (Σ) replaces the exchange-correlation energy in DFT. The self-energy operator is then approximated as a product of Green's function (G) and screened Coulomb interaction (W) [30]. In the present implementation, the GW approximation is applied perturbatively to the DFT wave functions and one-electron energy. This leads to several different GW approaches depending on whether these quantities in G and W operators are iterated self-consistently or not. The most basic level is G_0W_0, which corrects the initial DFT eigenvalues using only one-shot perturbation. In typical main-group semiconductors or oxides such as Si or MgO, it was found that the G_0W_0 calculation considerably improves the band gap in comparison with DFT results, although substantial underestimations still remain [31]. GW calculations with higher self-consistency level are divided into two groups. One is the eigenvalue-only updated approach such as GW_0 or GW calculations. In the other style called $QPGW_0$ or $QPGW$ calculations, quasiparticle wave functions as well as eigenvalues are updated. The difference between $QPGW_0$ and $QPGW$ (or GW_0 and GW) is whether the self-consistency in the eigenvalues is considered only in G ($QPGW_0$ and GW_0) or both G and W ($QPGW$ and GW). From the numerous tests on various material classes, a consensus seems to arise that overall, the GW_0 scheme produces results that are closest to the experimental band gaps [32,33].

For TiO_2 and $SrTiO_3$, there have been plenty of GW studies. In the case of rutile TiO_2, the G_0W_0 band gaps are reported to be 3.34 ∼ 3.79 eV [26,34–37] that are larger than 3.3 eV obtained from photoemission measurement or 3.03 eV from optical measurement [25,38,39]. Such an overestimation in G_0W_0 calculation has not been observed in sp semiconductors for which the band gap is typically underestimated [31]. Eigenvalue-updated self-consistent GW calculation increases the band gap even further to 4.48 eV [40], making the discrepancy with experiment even larger. The band gap of rutile TiO_2 within $QPGW$ is reported as 3.78 eV [41], which is smaller than the GW result but still bigger than the experimental value. For $SrTiO_3$, previous quasiparticle calculations reported the quasiparticle band gap as 3.36 ∼ 5.07 eV (G_0W_0) and 4.19 eV ($QPGW$) [27,41–44], while the experimental photoemission spectroscopy on $SrTiO_3$ gives

*hansw@snu.ac.kr

the gap of ∼3.3 eV [25,45]. The GW calculation on anatase TiO_2 has been limited only to the G_0W_0 level as far as we are aware, and the computed band gaps range from 3.56 to 4.29 eV [26,34–37,46].

Overall, the G_0W_0 calculations on titanates overestimate the band gap slightly, and further iteration of self-consistency cycle in G and W widened the band gap, worsening the agreement with experiment. This is a conclusion that is markedly different from other main-group insulators for which G_0W_0 underestimates the band gap and GW_0 results show good agreements with experiment. In Ref. [40], large errors were noted for GW results on transition-metal oxides in general, and the additional on-site potential on the d orbital was introduced to improve the band gap. However, the empirical nature of the on-site potential may limit its predictive capability.

In this article, we systematically test all levels of GW calculations on rutile and anatase TiO_2 and simple cubic $SrTiO_3$ with an aim to establish a proper GW scheme that can be applied to titanates in d^0 configurations. We also carefully test computational parameters in GW approximations such as energy cutoff for the plane wave basis, **k**-point sampling, number of unoccupied bands, and frequency grids. It turns out that for all the titanates considered, the QPG_0W_0 scheme which maintains the dielectric screening to that from the initial PBE functional while wave functions are updated self-consistently, improves the band gaps over any other GW scheme, resulting in the agreement with experiment with less than ∼10% error.

The rest of this article is organized as follows: In Sec. II, we discuss the computational methods and test the convergence with respect to computational parameters. The main results are discussed in Sec. III, and Sec. IV summarizes and concludes the present work.

II. COMPUTATIONAL METHODS

A. Computational setup

The DFT and GW calculations are performed using the Vienna *ab initio* simulation package (VASP) with the projector-augmented wave (PAW) method [47–49]. We use experimental lattice structures and atomic positions for every material [50,51]. The crystal structures of rutile, anatase, and $SrTiO_3$ and their lattice parameters are shown in Fig. 1. Initial eigenvalues and eigenfunctions are calculated within PBE-based generalized gradient approximation [52], and the energy cutoff of 500 eV is used for the plane-wave basis to expand the wave functions. We include $3s$ and $3p$ semicore electrons in the valence configuration of Ti, since they considerably influence the DFT ground states and quasiparticle energy levels [26]. In our own tests using G_0W_0, it is found that the exclusion of the semicore state increases the quasiparticle band gap by 0.3 eV. We use PAW potentials that are constructed to yield accurate scattering properties in the high-energy range [31,53]. The dynamical dielectric matrix that screens Coulomb interaction is evaluated within the random-phase approximation.

B. Convergence test and parameter fitting

It is well known that the results of GW calculations are significantly affected by computational parameters, such as

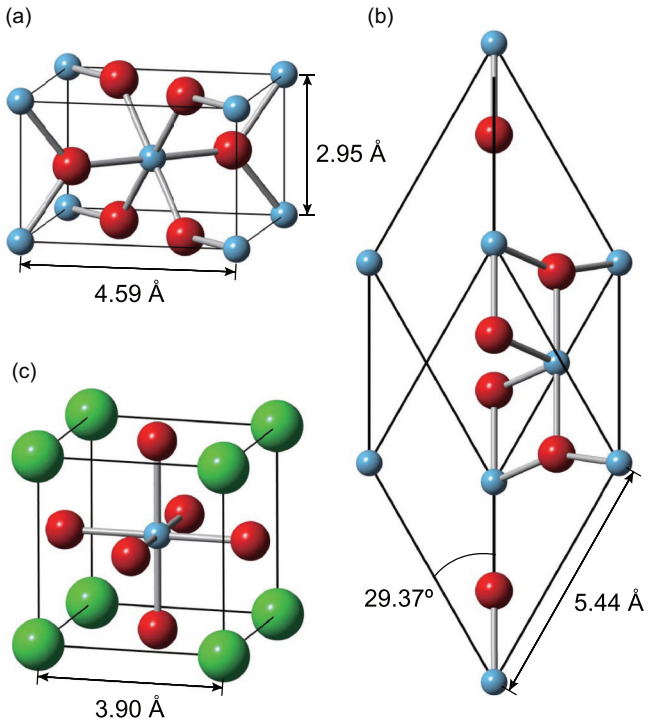

FIG. 1. (Color online) The primitive cell structures of (a) rutile TiO_2, (b) anatase TiO_2, and (c) $SrTiO_3$. The largest (green), medium (red), and the smallest (sky-blue) balls indicate Sr, O, and Ti atoms, respectively.

energy cutoff for the plane-wave basis set, **k**-point sampling, and the number of unoccupied states. To examine the convergence with respect to these parameters, we systematically perform test G_0W_0 calculations for each titanate. The results for rutile TiO_2 are shown in Fig. 2 as a representative case. The band-gap convergence with respect to the basis set is provided in Fig. 2(a), which shows that the energy cutoff of 500 eV gives the fully converged result. Figure 2(b) confirms that the (Γ-centered) 3 × 3×5 grid is sufficient to produce converged band gaps within 0.1 eV. For anatase and $SrTiO_3$, 4 × 4×4 and 6 × 6×6 give the converged results. As to the number of unoccupied states, the band gap is slowly converged as shown in Fig. 2(c). However, the band gap can be linearly fitted against the inverse of the number of bands ($1/N_b$) and this allows for using a manageable number of N_b (see below). Such behaviors were also observed in other materials [26,54].

The number of energy grid (N_ω) used in sampling the dielectric screening function in the self-energy is also a critical parameter. To be specific, the diagonal component of frequency-dependent self-energy Σ is formulated as follows:

$$\Sigma(\omega)_{n\mathbf{k},n\mathbf{k}} = \frac{1}{\Omega}\sum_{\mathbf{q}\mathbf{G}\mathbf{G}'}\sum_{n'}\frac{i}{2\pi}\int_{-\infty}^{\infty}d\omega' W(\mathbf{G}+\mathbf{q},\mathbf{G}'+\mathbf{q},\omega') \times \frac{\langle\psi_{n\mathbf{k}}|e^{i(\mathbf{q}+\mathbf{G})\cdot\mathbf{r}}|\psi_{n'\mathbf{k}-\mathbf{q}}\rangle\langle\psi_{n'\mathbf{k}-\mathbf{q}}|e^{-i(\mathbf{q}+\mathbf{G}')\cdot\mathbf{r}'}|\psi_{n\mathbf{k}}\rangle}{\omega+\omega'-\epsilon_{n'\mathbf{k}-\mathbf{q}}+i\eta\mathrm{sgn}[\epsilon_{n'\mathbf{k}-\mathbf{q}}-\mu]}, \quad (1)$$

where Ω is the cell volume, $\mathbf{G}(\mathbf{q})$ is the reciprocal lattice (Bloch) vectors, μ is the Fermi energy, and η means an

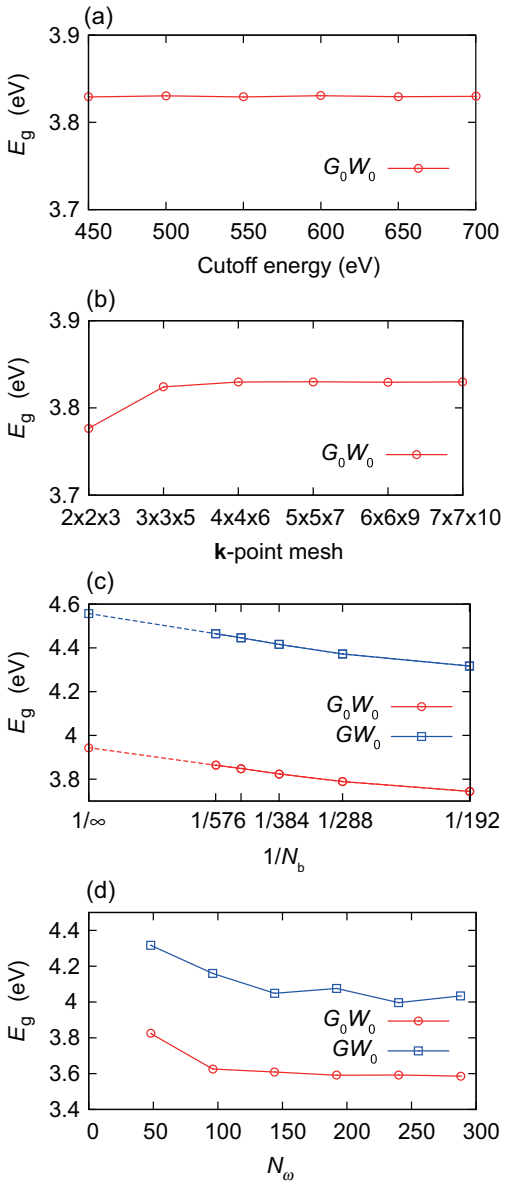

FIG. 2. (Color online) The G_0W_0 (circles) and GW_0 (squares) band gaps of rutile with respect to (a) energy cutoff, (b) **k**-point mesh, (c) the inverse of the number of bands ($1/N_b$), and (d) the number of frequency grids (N_ω). Dashed lines in (c) are the linear extrapolation from calculated data.

infinitesimal broadening. In Eq. (1), $\psi_{n\mathbf{k}}$ and $\epsilon_{n\mathbf{k}}$ are the wave function and eigenvalue of the state with band index n and Bloch vector **k**, respectively. The integration over ω' in Eq. (1) is replaced by the weighted summation over N_ω grid points along the frequency axis. (See Ref. [31] for the details of the sampling method.) Since we included $3s$ and $3p$ semicore states of Ti as valence electrons, the frequency grid should be sampled at larger magnitudes of ω' than for typical materials, which increases N_ω. Figure 2(d) shows the convergence with respect to N_ω, which shows that $N_\omega = 48$, a reasonable value for conventional sp semiconductors, is clearly not enough.

In the above, N_b and N_ω required for the fully converged results are too high within our computational resources. In order to make the computation feasible, we use $N_\mathrm{b} = 384$ and $N_\omega = 48$ for every GW scheme and add a correction term that corresponds to the difference in G_0W_0 results between this parameter set and $N_\mathrm{b} = \infty$, and $N_\omega = 288$. This assumes that the convergence behavior is similar among different GW schemes. To confirm this, we carry out GW_0 calculations in Figs. 2(c) and 2(d). It is seen that the GW_0 results show similar convergence behaviors in the quasiparticle band gap. The gap correction for each titanate is summarized in Table I.

TABLE I. The correction term added to each GW result obtained with 384 and 48 for the number of bands and frequency grids, respectively. ΔE_band (ΔE_grid) reflects the misconvergence in the number of bands (frequency grids). ΔE_tot is the summation of the two terms. The unit is eV.

	ΔE_bands	ΔE_grids	ΔE_tot
Rutile	0.120	−0.238	−0.118
Anatase	0.135	−0.186	−0.051
$SrTiO_3$	0.117	−0.200	−0.083

III. RESULTS AND DISCUSSIONS

A. Calculated quasiparticle band gap

The band gaps of TiO_2 and $SrTiO_3$ within various GW schemes are presented in Table II. The errors in reference to the experimental data are displayed in Fig. 3. In the case of self-consistent GW schemes, the iterations are repeated until the band gap is converged within 0.01 eV. The experimental band gaps of rutile TiO_2 and the $SrTiO_3$ were measured by photoemission spectroscopy [25,45], and directly compare with the present GW results that neglect excitonic effects. On the other hand, the available data of anatase TiO_2 was measured by optical measurement [56], and photoemission data have not been reported as far as we are aware. The calculated exciton binding energy for anatase is known to be 0.16 eV [35], and so this could be added to the optical gap for the fair comparison.

In Table II and Fig. 3, the band gaps from the PBE functional are significantly underestimated compared to the experimental value, which is the well-known shortcoming of the semilocal functionals. In the G_0W_0 calculations, the band gaps are overcorrected and bigger than the experimental values. The

TABLE II. The quasiparticle band gaps calculated within the PBE exchange-correlation functional and various GW schemes. In parentheses are band gaps from previous studies. Values from experimental measurements are also presented. The unit of energy is eV.

	PBE	G_0W_0	GW_0	GW	$QPGW_0$	$QPGW$	Expt.
Rutile	1.87	3.66 (3.46)[a]	4.23	4.84	3.39	3.85 (3.82)[b]	3.3[c]
Anatase	2.17	4.03 (3.73)[a]	4.60	5.28	3.79	4.12	3.4[d]
$SrTiO_3$	1.88	3.83 (3.82)[e]	4.43	5.08	3.67	3.88 (4.12)[b]	3.3[f]

[a]Reference [35].
[b]Reference [41].
[c]Reference [25] (photoemission).
[d]Reference [56] (optical).
[e]Reference [42].
[f]Reference [45] (photoemission).

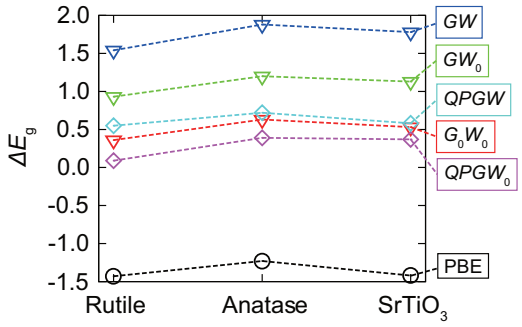

FIG. 3. (Color online) The error in the band gap (ΔE_g) with respect to the measured values of rutile, anatase, and $SrTiO_3$.

eigenvalue-updated self-consistent calculation such as GW_0 or GW increases the band gap further, worsening the agreement with the experimental value. In particular, GW results show the biggest discrepancy with the error of 47%, 55%, and 54% for rutile, anatase, and $SrTiO_3$, respectively. It is noted that the overestimation is reduced considerably in $QPGW_0$, leading to the best agreement with experiments. With $QPGW$, corresponding to the highest self-consistency level, the band-gap overestimation is bigger than $QPGW_0$ or G_0W_0.

It is known that the quasipartcle band gap can be affected by the pseudopotential method. To check this, we compare the present data with the all-electron $QPGW$ results in Ref. [41] that were based on the linearized augmented-plane-wave (LAPW) method (see Table II). The band-gap differences with respect to the present result are 0.03 eV for rutile and 0.24 eV for $SrTiO_3$. While the band gaps of $SrTiO_3$ show some discrepancy, it is also overestimated in the all-electron calculations.

We also computed G_0W_0 results with the starting functional as the HSE-type hybrid functional since this is a favored recipe in literature [35,57,58]. The computed results are 3.82 eV, 4.28 eV, and 5.15 eV for rutile, anatase, and $SrTiO_3$, respectively. Therefore, the one-shot G_0W_0 on top of HSE results does not produce satisfactory results on titanates.

When comparing the difference between the schemes updating the dielectric function and fixing the screening to the initial DFT forms (i.e., GW_0 with GW or $QPGW_0$ with $QPGW$), the former consistently yields better agreements with experimental data. This is a result of error cancellation between the overestimated dielectric polarizability of random phase approximation and the underestimated band gap of DFT [32,59]. If we update the eigenvalues in the dielectric function, the energy gap increases and the dielectric constant is underestimated, resulting in the overestimation of the band gap. To be specific, the macroscopic dielectric constant calculated by GW and $QPGW$ are 5.25 and 4.86, respectively, which is smaller than the experimental values of 7.37 [60]. The dielectric constant from PBE is 7.50, which is in fair agreement with experiment. In the following discussions, we mainly discuss GW_0 and $QPGW_0$ results.

Comparing the result of GW_0 and $QPGW_0$, it is found that the wave-function update reduces the band gap by ~0.8 eV consistently for every titanate, improving the band gap significantly. This is in contrast to the case of typical

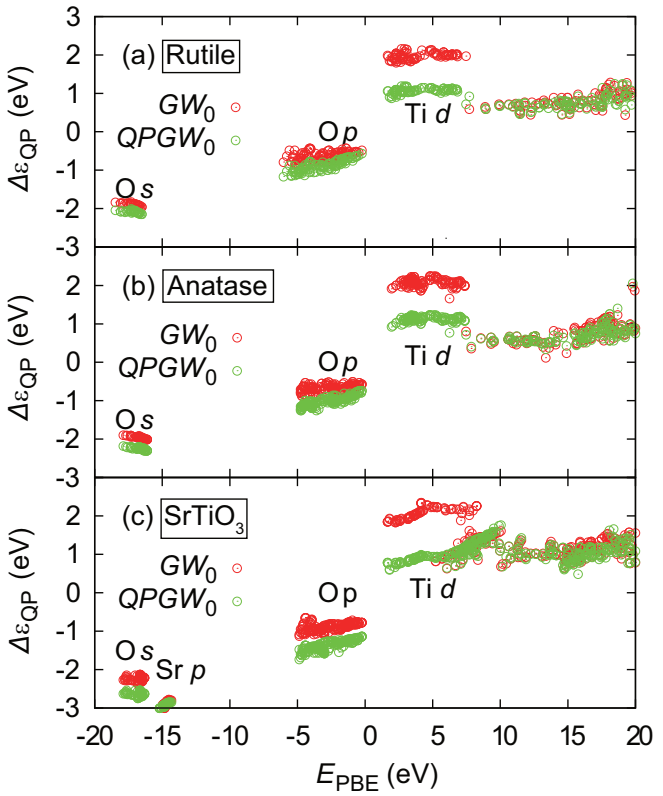

FIG. 4. (Color online) The quasiparticle shift ($\Delta\epsilon_{QP}$) with respect to the DFT eigenvalue is presented for (a) rutile, (b) anatase, and (c) $SrTiO_3$. The Fermi level is set to zero.

sp semiconductors [32] and post-transition-metal oxides [33], in which eigenvalue-only updated GW_0 calculation yields the best agreements with experiment, and the wave-function update in $QPGW_0$ slightly overestimates the band gap. The large change in the quasiparticle levels in titanates indicates that the electron density is significantly affected by the wave-function update. The detailed analysis on this will be provided in the Sec. III C.

B. Quasiparticle shift and band structure

In Fig. 4, the quasiparticle shifts of GW_0 and $QPGW_0$ with respect to the initial PBE eigenvalues are presented. The dominant orbital character is noted on each subband. It is seen that the GW_0 calculations shift all the subbands significantly: The Ti-d orbital which forms the conduction band minimum is shifted upward by ~2 eV while the O-p orbital in the valence band is shifted downward by 0.5–1 eV. The quasiparticle shift in the opposite directions between occupied and unoccupied bands accounts for the band-gap widening in GW_0. When the wave functions are updated self-consistently in $QPGW_0$, every quasiparticle level shifts down additionally. The down-shift is more pronounced for Ti-d orbitals than for the O-p orbitals, resulting in the band-gap narrowing in $QPGW_0$. Further discussions on this will be given in the next session.

The band structures of rutile and $SrTiO_3$ obtained from GW approximations are provided in Fig. 5. To obtain the quasiparticle levels at **k** points that were not sampled in the DFT calculations, the maximally localized Wannier

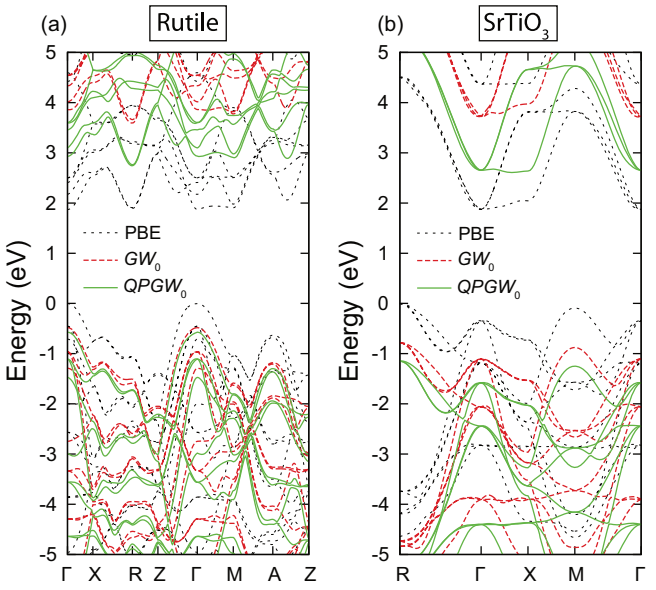

FIG. 5. (Color online) Band structures of (a) rutile and (b) $SrTiO_3$. The dotted (gray), dashed (red), and solid (green) lines indicate PBE, GW_0, and $QPGW_0$ results, respectively. The Fermi level is set to zero.

functions are used, which are constructed from the GW wave functions by the WANNIER90 code [61]. Figure 5 shows that the GW calculation widens the band gap in comparison to the PBE results, but the overall dispersion and the widths of conduction and valence bands are well maintained regardless of computational scheme. Nevertheless, the conduction-band bottoms are almost degenerate along $\Gamma - M$ and at R for rutile, and along $\Gamma - X$ for $SrTiO_3$, and the fine energy ordering among these **k** points slightly changes with GW approximations; in rutile TiO_2, GW_0 and $QPGW_0$ shift the conduction band minimum from Γ to R. That is to say, PBE gives the direct band gap while GW_0 and $QPGW_0$ approximations result in the indirect band gap. This is consistent with previous GW studies [26]. On the other hand, the conduction minimum of $SrTiO_3$ is altered from Γ to X in $QPGW_0$ results but the band-gap nature is always indirect.

Experiments show that rutile has a direct band gap of ~3.0 eV and indirect band gap of ~3.1 eV [38,62,63]. Therefore, the band-gap nature is at variance with the present GW results that conclude the indirect band gap. However, we also note that the difference between the direct and indirect band gaps is only 0.17 eV in $QPGW_0$. In the case of $SrTiO_3$, an indirect band gap of 3.2 eV was first suggested by Cardona [64] and supported by other works [65–67]. The direct gap was reported to be 3.4–3.8 eV [65–67]. Therefore, the difference between the direct and indirect band gaps is 0.2–0.6 eV, and this is consistent with the $QPGW_0$ difference of 0.47 eV in Fig. 5(b).

C. Effects of wave-function updates

As shown in the above, the band gaps are significantly reduced when the wave functions are updated self-consistently, which is contrary to the usual observations in GW calculations. To reveal the origin of this, we plot in Fig. 6(a) the electron density difference of rutile TiO_2 between $QPGW_0$ and PBE

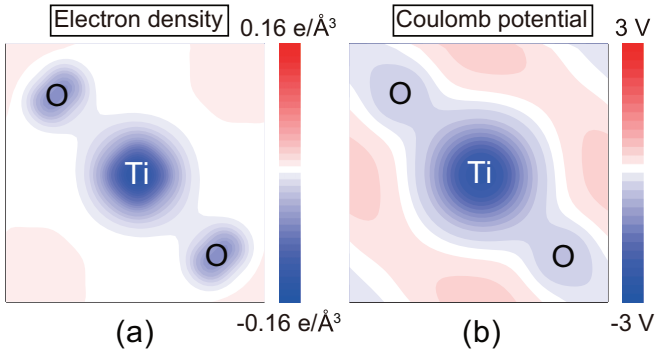

FIG. 6. (Color online) The difference in (a) the electron density and (b) the Coulomb potential between PBE and $QPGW_0$ results on rutile TiO_2.

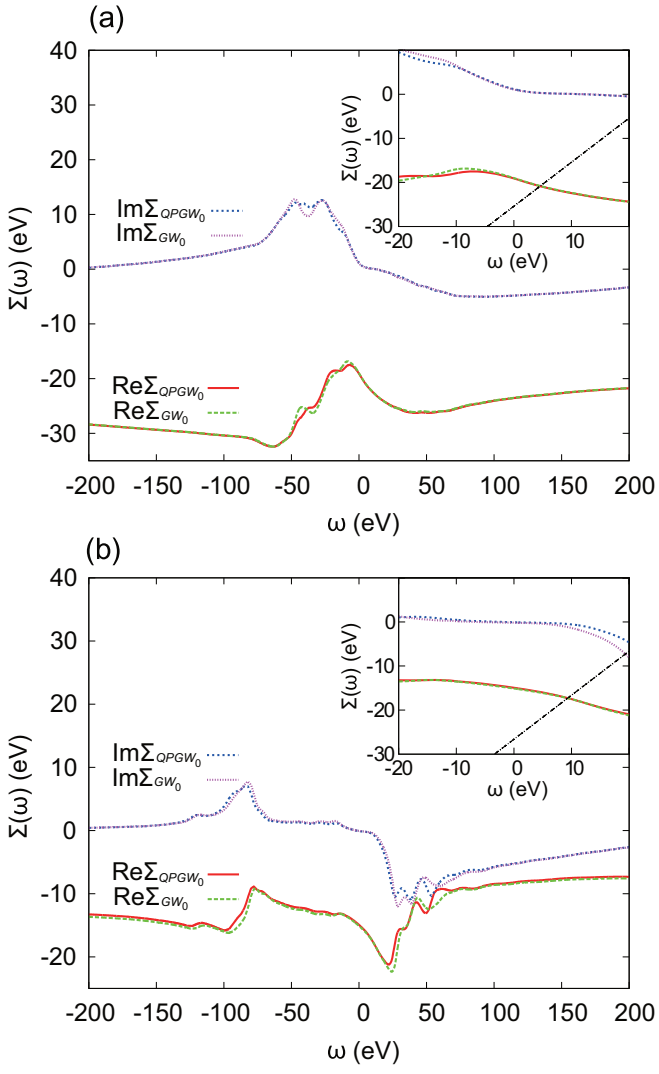

FIG. 7. (Color online) The real and imaginary parts of the self-energy for the states at (a) valence band maximum (VBM) and (b) conduction band minimum (CBM) (at Γ) in rutile. Insets are given for the smaller range of frequency. The black dashed-dot line is shown for $\omega - \epsilon_{\text{no-ex}}$, where $\epsilon_{\text{no-ex}}$ indicates the eigenvalue without exchange correlation of DFT. In the insets, intersections with Re[Σ] correspond to the self-energy at the quasiparticle peak.

calculations. After self-consistency cycles, the wave functions slightly spread out from atomic sites to the vacant interstitial space between atoms, reducing the electron density close to the ions. The corresponding change in the Coulomb potential in Fig. 6(b) shows that the electrostatic repulsion is reduced near the atomic sites. This shifts down the energy levels of both Ti-d and O-p orbitals, which is consistent with Fig. 4. In Fig. 6, it is seen that the reduction in the electron density and Coulomb potential is more pronounced at Ti than O sites. This lowers the quasiparticle levels of the Ti-d orbital further than O-p orbitals, resulting in the significant band-gap reduction as shown in Fig. 4. Similar changes in electron density and Coulomb potential also occur for anatase and cubic $SrTiO_3$. Interestingly, similar analysis in Ref. [33] on post-transition metal oxides such as ZnO, Ga_2O_3, In_2O_3, and SnO_2, exhibits different results; in these materials, the density reduction after wave-function updates is larger at oxygen sites than metal sites, and the quasiparticle band gap increases because the conduction bands consist of metal s orbitals.

In Fig. 7, real and imaginary parts of the self-energy for the states at valence and conduction edges are plotted for rutile. The imaginary part of self-energy means the inverse of the lifetime of the quasiparticle, which is finite in the interacting system. The real part of self-energy will give the excitation energy of the electron if added to the noninteracting Hamiltonian [55]. No significant difference is noticeable between GW_0 and $QPGW_0$ results, which implies that the noninteracting Hartree potential plays an important role in electronic structure change.

IV. SUMMARY

In summary, we analyzed the electronic structure of rutile, anatase, and $SrTiO_3$ by employing various types of GW calculations. We paid special attention to the convergence behavior of computational parameters such as **k** points, the number of bands, and frequency grids in self-energy, and reported quasiparticle band gaps that are fully converged. We found that while the GW_0, GW, and $QPGW$ calculations overestimate the band gap significantly, the $QPGW_0$ scheme gives the best results that agree with the experimental data within ∼10% error. It was found that the wave-function updates in $QPGW_0$ and $QPGW$ reduce the electronic density near the atomic sites, more so at Ti than O sites, which contributes to reducing the band gap that is overestimated by GW and GW_0. We believe that the present work can serve as a good starting point to studies where the correct description of the band gap of titanates is a crucial issue. In future study, we are going to expand the material system to other transition metal oxides to investigate whether similar effects are observed.

ACKNOWLEDGMENTS

This research was supported by the EDISON program through the Ministry of Science, ICT and Future Planning, National Research Foundation of Korea (NRF-2012M3C1A6035307). The computations were carried out at KISTI supercomputing center (KSC-2014-C3-012).

[1] F. Grant, Rev. Mod. Phys. **31**, 646 (1959).
[2] A. Fujishima and K. Honda, Nature (London) **238**, 37 (1972).
[3] B. O'Regan and M. Grätzel, Nature (London) **353**, 737 (1991).
[4] A. Kahn and A. Leyendecker, Phys. Rev. **135**, A1321 (1964).
[5] J. Haeni, P. Irvin, W. Chang, R. Uecker, and P. Reiche, Nature (London) **430**, 758 (2004).
[6] S. U. M. Khan, M. Al-Shahry, and W. B. Ingler, Science **297**, 2243 (2002).
[7] M. Ni, M. K. H. Leung, D. Y. C. Leung, and K. Sumathy, Renew. Sustain. Energy Rev. **11**, 401 (2007).
[8] U. Bach, D. Lupo, P. Comte, and J. Moser, Nature (London) **395**, 583 (1998).
[9] G. K. Mor, K. Shankar, M. Paulose, O. K. Varghese, and C. A. Grimes, Nano Lett. **6**, 215 (2006).
[10] S. Kim, M. Son, S. Park, M. Jeong, H. Seo, K. Prabakar, and H. Kim, Electron. Mater. Lett. **10**, 229 (2014).
[11] T. Bui, T. Matrab, V. Woehling, J. Longuet, C. Plesse, G. T. M. Nguyen, F. Vidal, and F. Goubard, Electron. Mater. Lett. **10**, 209 (2014).
[12] A. Ohtomo and H. Y. Hwang, Nature (London) **427**, 423 (2004).
[13] L. Li, C. Richter, J. Mannhart, and R. C. Ashoori, Nat. Phys. **7**, 762 (2011).
[14] J. A. Bert, B. Kalisky, C. Bell, M. Kim, Y. Hikita, H. Y. Hwang, and K. A. Moler, Nat. Phys. **7**, 767 (2011).
[15] D. A. Dikin, M. Mehta, C. W. Bark, C. M. Folkman, C. B. Eom, and V. Chandrasekhar, Phys. Rev. Lett. **107**, 056802 (2011).
[16] A. Kalabukhov, R. Gunnarsson, J. Börjesson, E. Olsson, T. Claeson, and D. Winkler, Phys. Rev. B **75**, 121404 (2007).
[17] W.-J. Son, E. Cho, B. Lee, J. Lee, and S. Han, Phys. Rev. B **79**, 245411 (2009).
[18] D. Fuchs, C. W. Schneider, R. Schneider, and H. Rietschel, J. Appl. Phys. **85**, 7362 (1999).
[19] J. Robertson, Rep. Prog. Phys. **69**, 327 (2006).
[20] S. W. Lee, O. S. Kwon, J. H. Han, and C. S. Hwang, Appl. Phys. Lett. **92**, 222903 (2008).
[21] S. Kim, G.-J. Choi, S. Lee, M. Seo, S. W. Lee, J. Han, H.-S. Ahn, S. Han, and C. S. Hwang, Adv. Mater. **20**, 1429 (2008).
[22] A. J. Cohen, P. Mori-Sánchez, and W. Yang, Science **321**, 792 (2008).
[23] A. J. Cohen, P. Mori-Sánchez, and W. Yang, Phys. Rev. B **77**, 115123 (2008).
[24] P. Mori-Sánchez, A. J. Cohen, and W. Yang, Phys. Rev. Lett. **100**, 146401 (2008).
[25] Y. Tezuka, S. Shin, T. Ishii, and T. Ejima, J. Phys. Soc. Jpn. **63**, 347 (1994).
[26] W. Kang and M. S. Hybertsen, Phys. Rev. B **82**, 085203 (2010).
[27] C. Friedrich, S. Blügel, and A. Schindlmayr, Phys. Rev. B **81**, 125102 (2010).
[28] P. Deák, B. Aradi, and T. Frauenheim, Phys. Rev. B **83**, 155207 (2011).
[29] F. Da Pieve, S. Di Matteo, T. Rangel, M. Giantomassi, D. Lamoen, G.-M. Rignanese, and X. Gonze, Phys. Rev. Lett. **110**, 136402 (2013).
[30] L. Hedin, Phys. Rev. **139**, A796 (1965).
[31] M. Shishkin and G. Kresse, Phys. Rev. B **74**, 035101 (2006).
[32] M. Shishkin and G. Kresse, Phys. Rev. B **75**, 235102 (2007).

[33] Y. Kang, G. Kang, H. H. Nahm, S. H. Cho, Y. S. Park, and S. Han, Phys. Rev. B **89**, 165130 (2014).
[34] C. E. Patrick and F. Giustino, J. Phys. Condens. Matter **24**, 202201 (2012).
[35] M. Landmann, E. Rauls, and W. G. Schmidt, J. Phys. Condens. Matter **24**, 195503 (2012).
[36] L. Chiodo, J. M. García-Lastra, A. Iacomino, S. Ossicini, J. Zhao, H. Petek, and A. Rubio, Phys. Rev. B **82**, 045207 (2010).
[37] L. Thulin and J. Guerra, Phys. Rev. B **77**, 195112 (2008).
[38] J. Pascual, J. Camassel, and H. Mathieu, Phys. Rev. Lett. **39**, 1490 (1977).
[39] A. Amtout and R. Leonelli, Phys. Rev. B **51**, 6842 (1995).
[40] S. Lany, Phys. Rev. B **87**, 085112 (2013).
[41] M. van Schilfgaarde, T. Kotani, and S. Faleev, Phys. Rev. Lett. **96**, 226402 (2006).
[42] A. R. Benrekia, N. Benkhettou, A. Nassour, M. Driz, M. Sahnoun, and S. Lebègue, Physica B **407**, 2632 (2012).
[43] G. Cappellini, J. Phys. Condens. Matter **12**, 3671 (2000).
[44] L. Sponza, V. Véniard, F. Sottile, C. Giorgetti, and L. Reining, Phys. Rev. B **87**, 235102 (2013).
[45] M. Takizawa, K. Maekawa, H. Wadati, T. Yoshida, A. Fujimori, H. Kumigashira, and M. Oshima, Phys. Rev. B **79**, 113103 (2009).
[46] P. Umari, L. Giacomazzi, F. De Angelis, M. Pastore, and S. Baroni, J. Chem. Phys. **139**, 014709 (2013).
[47] P. E. Blöchl, Phys. Rev. B **50**, 17953 (1994).
[48] G. Kresse and D. Joubert, Phys. Rev. B **59**, 1758 (1999).
[49] G. Kresse and J. Furthmuller, Phys. Rev. B **54**, 11169 (1996).
[50] J. Burdett and T. Hughbanks, J. Am. Chem. Soc. **109**, 3639 (1987).
[51] Yu. A. Abramov, V. G. Tsirelson, V. E. Zavodnik, S. A. Ivanov, and I. D. Brown, Acta Crystallogr. Sect. B **51**, 942 (1995).
[52] J. P. Perdew, K. Burke, and M. Ernzerhof, Phys. Rev. Lett. **77**, 3865 (1996).
[53] G. Kresse, M. Marsman, L. E. Hintzsche, and E. Flage-Larsen, Phys. Rev. B **85**, 045205 (2012).
[54] C. Friedrich, M. C. Müller, and S. Blügel, Phys. Rev. B **83**, 081101(R) (2011).
[55] F. Aryasetiawan and O. Gunnarsson, Rep. Prog. Phys. **61**, 237 (1998).
[56] H. Tang, F. Lévy, H. Berger, and P. E. Schmid, Phys. Rev. B **52**, 7771 (1995).
[57] S. Lany and A. Zunger, Phys. Rev. B **81**, 113201 (2010).
[58] L. Y. Isseroff and E. A. Carter, Phys. Rev. B **85**, 235142 (2012).
[59] M. Shishkin, M. Marsman, and G. Kresse, Phys. Rev. Lett. **99**, 246403 (2007).
[60] J. G. Traylor, H. G. Smith, R. M. Nicklow, and M. K. Wilkinson, Phys. Rev. B **3**, 3457 (1971).
[61] A. A. Mostofi, J. R. Yates, Y.-S. Lee, I. Souza, D. Vanderbilt, and N. Marzari, Comput. Phys. Commun. **178**, 685 (2008).
[62] A. Welte, C. Waldauf, C. Brabec, and P. J. Wellmann, Thin Solid Films **516**, 7256 (2008).
[63] J. Pascual, J. Camassel, and H. Mathieu, Phys. Rev. B **18**, 5606 (1978).
[64] M. Cardona, Phys. Rev. **140**, A651 (1965).
[65] D. Goldschmidt and H. L. Tuller, Phys. Rev. B **35**, 4360 (1987).
[66] S. Zollner, A. A. Demkov, R. Liu, P. L. Fejes, R. B. Gregory, Prasad Alluri, J. A. Curless, Z. Yu, J. Ramdani, R. Droopad, T. E. Tiwald, J. N. Hilfiker, and J. A. Woollam, J. Vac. Sci. Technol. B **18**, 2242 (2000).
[67] K. van Benthem, C. Elsässer, and R. H. French, J. Appl. Phys. **90**, 6156 (2001).